

Risk assessment of post-wildfire hydrological response in semiarid basins: the effects of varying rainfall representations in the KINEROS2/AGWA model

Gabriel Sidman^{A,C}, D. Phillip Guertin^A, David C. Goodrich^B,
Carl L. Unkrich^B and I. Shea Burns^A

^ASchool of Natural Resources and the Environment, University of Arizona, 1311 East 4th Street, Suite 325, Tucson, AZ 85721, USA.

^BSouthwest Watershed Research Center, USDA-ARS, 2000 East Allen Rd, Tucson, AZ 85719, USA.

^CCorresponding author. Email: gabriel.sidman@winrock.org

Abstract. Representation of precipitation is one of the most difficult aspects of modelling post-fire runoff and erosion and also one of the most sensitive input parameters to rainfall-runoff models. The impact of post-fire convective rainstorms, especially in semiarid watersheds, depends on the overlap between locations of high-intensity rainfall and areas of high-severity burns. One of the most useful applications of models in post-fire situations is risk assessment to quantify peak flow and identify areas at high risk of flooding and erosion. This study used the KINEROS2/AGWA model to compare several spatial and temporal rainfall representations of post-fire rainfall-runoff events to determine the effect of differing representations on modelled peak flow and determine at-risk locations within a watershed. Post-fire rainfall-runoff events at Zion National Park in Utah and Bandelier National Monument in New Mexico were modelled. Representations considered included both uniform and Soil Conservation Service Type II hyetographs, applying rain over the entire watershed and applying rain only on the burned area, and varying rainfall both temporally and spatially according to radar data. Results showed that rainfall representation greatly affected modelled peak flow, but did not significantly alter the model's predictions for high-risk locations. This has important implications for post-fire assessments before a flood-inducing rainfall event, or for post-storm assessments in areas with low-gauge density or lack of radar data due to mountain beam blockage.

Additional keywords: Bandelier National Monument, design storm, peak flow, radar, rainfall representation, Zion National Park.

Received 2 May 2014, accepted 7 March 2015, published online 7 July 2015

Introduction

Representing rainfall in hydrological modelling

Inaccurately representing rainfall has been identified as one of the largest sources of error in hydrological models used for flood prediction (Woolhiser and Goodrich 1988; Yatheendradas *et al.* 2008; Schröter *et al.* 2011). This is especially true in regions where small convective storms dominate rainfall regimes (Goodrich *et al.* 1997). In these regions, rainfall can vary greatly both spatially and temporally during the course of a storm, which can be difficult to represent in a model. Temporal representations for many rainfall-runoff models and rainfall simulator experiments use constant intensity throughout the course of a storm, which has proved to be unrepresentative of reality (Dunkerley 2012). Storms represented with constant-intensity hyetographs have been found to underpredict peak discharge, whereas triangular hyetographs tend to overpredict peak discharge (Lambourne and Stephenson 1987).

Furthermore, efforts to disaggregate daily rainfall amounts have proved to distort runoff values greatly, making it difficult to use poor-resolution rainfall data (Woolhiser and Goodrich 1988). Spatial representation of rainfall can also be difficult for hydrological models. The most basic way to model rainfall is to apply it spatially uniformly over the entire watershed. This method has been proved to be a poor representation for convective storms even in small watersheds (Milly and Eagleson 1988; Faurès *et al.* 1995; Goodrich *et al.* 1995). Efforts to address this problem have included using area reduction factors, which often do not take storm type into account (Wright *et al.* 2014), and interpolation, which depends on a dense network of rain gauges (García *et al.* 2008). Temporal and spatial aspects of rainfall are interrelated in many ways as well (Moody *et al.* 2013). The movement of a storm cell and its location in the watershed at moments of peak rainfall intensity are critical factors in determining runoff response (Singh 1998).

Newer models have attempted to solve rainfall representation issues by harnessing outputs from radar products (Singh and Woolhiser 2002; Hardegree *et al.* 2003). Although use of radar products allows more dynamic spatial and temporal characterisation, many of the most commonly used products have their own sources of error and require storm-by-storm calibration (Morin *et al.* 2006; Schröter *et al.* 2011). Hossain *et al.* (2004) found that in mountainous terrain, modelled runoff predictions using radar representation were approximately equal to those using a dense rain gauge network if radar rainfall observations were calibrated using rain gauge data. Recent radar products such as those using dual-polarimetric-derived rainfall intensity, when also calibrated, improve runoff prediction, especially when deployed in close proximity to the watershed (Jorgensen *et al.* 2011). Newer methods of spatial downscaling have also shown promise in improving radar estimations of peak rainfall locations (Tao and Barros 2010).

Rainfall representation for post-fire runoff prediction

In the southwestern United States, the convective storms associated with the monsoon season can cause damaging floods because they follow directly after the dry, hot summer period with many wildfires. Post-fire flooding and erosion that result from these convective storms have become a focus of hydrological modellers and emergency response teams in order to better predict the magnitude of such events and watershed areas at risk (Foltz *et al.* 2009). From a temporal context, accurate post-fire modelling can be especially difficult because peak discharge and debris flows are correlated with very short bursts of high rainfall intensity (Cannon *et al.* 2008; Kean *et al.* 2011; Moody 2011). From a spatial context, damaging post-fire runoff and erosion are common in small mesoscale watersheds following short convective rainstorms (Moody *et al.* 2013). There is also evidence that a complex set of factors at the meso-scale (including reduced albedo, planetary boundary layer instability and moisture availability) can induce storm cell formation on burned areas, making burned areas more at risk for rain than unburned areas (Banta and Barker Schaaf 1987; Chen *et al.* 2001; Tryhorn *et al.* 2008).

Post-fire runoff prediction

Post-fire events are especially dangerous from a forecasting perspective because floods can occur in a burned watershed following small rainfall events that previously showed little hydrologic response when the watershed was unburned (Moody and Martin 2001). Emergency response efforts, such as those carried out by the Burned Area Emergency Response (BAER) teams that are tasked with predicting locations and magnitudes of post-fire flooding and erosion, utilise a variety of hydrological models and methods. These methods vary from simple empirical equations such as the United States Geological Survey (USGS) Regression method and the Rule of Thumb by Kuyumjian (Foltz *et al.* 2009), to physically based models such as the Erosion Risk Management Response Tool (ERMiT; Foltz *et al.* 2009) or the Kinematic Runoff and Erosion Model (KINEROS2; Goodrich *et al.* 2012).

The more basic methods calculate only a few metrics such as peak flow, and generally have a simplistic rainfall input.

They are useful for quick calculations or estimations, especially if the detail of input data needed to run the more complex physical models is not readily available. The USGS Regression and the Rule of Thumb by Kuyumjian methods require input of design storm intensity, duration, recurrence interval and ratio of post-fire to pre-fire runoff (Foltz *et al.* 2009). Because these methods are not spatial, it can be assumed that variation in rain across the watershed is not taken into account. Furthermore, with only one storm intensity given, temporal variation is also not considered. The analytical method of post-fire unit peak flow estimation described in Moody (2011) uses the maximum 30-min rainfall intensity, a more specific metric that has been correlated with post-fire peak flow. This method does not, however, include any spatial metrics for the rainfall input. The physically based Water Erosion Prediction Project (WEPP) model is used by ERMiT to predict the runoff and exceedance likelihood of different erosion rates (Robichaud *et al.* 2007). By using monthly climate station data for its precipitation input, which is then disaggregated into daily precipitation amounts, storm duration, time-to-peak and peak intensity are also derived. As ERMiT is designed for modelling at the hillslope scale, rainfall is assumed to be uniform over the modelled area.

KINEROS2 is another physically based model that predicts entire hydrographs and sedigraphs for a single rainfall event (Goodrich *et al.* 2012). Through the Automated Geospatial Watershed Assessment Tool (AGWA), KINEROS2 can be used to model watersheds on a meso-scale and break the watershed up into multiple channel and hillslope elements (Table 1). Users can choose to define a custom hyetograph or use a design storm, both of which can provide temporal resolution to the minute. KINEROS2/AGWA can provide spatially variable rainfall through the inclusion of data from multiple rain gauges throughout the watershed (Hernandez *et al.* 2000). In addition, a method was developed to allow input of National Climatic Data Center (NCDC) Level 3 digital hybrid reflectivity (DHR) radar data into KINEROS2 to potentially (depending on the number of comparison rain gauges) provide an even more realistic rainfall representation (Yatheendradas *et al.* 2008; Schaffner *et al.* 2010).

Although many studies have assessed the impact of varying rainfall representation on model prediction of runoff for unburned watersheds, none have examined burned watersheds where soil properties have been modified by wildfire. The present study utilises the KINEROS2/AGWA modelling tool to test how temporal and spatial variations of rainfall representation affect post-fire assessment of peak flow and sediment yield. When considering the impact of rainfall on the model's performance, two main goals of post-fire modelling are considered: reproducing the magnitude of a rainfall event's peak flow, and predicting the location of stream reaches and hillslopes at risk of flooding and erosion.

Methods

Study sites

Post-fire hydrological response was examined at two watersheds: North Creek within Zion National Park (ZION) in southwestern Utah, and Frijoles Canyon within Bandelier

Table 1. Key KINEROS2 default input parameters and their changes based on burn severity for major land-cover classes

Initial soil saturation, shown as the fraction of pore space filled, was 0.2. Saturated hydraulic conductivity was altered by the change in percentage cover. ZION, Zion National Park; BAND, Bandelier National Monument; DHR, digital hybrid reflectivity

Land cover	Hillslope percentage cover (%)			
	Unburned	Low severity	Moderate severity	High severity
Deciduous forest	50	43	34	25
Evergreen forest	50	43	34	25
Mixed forest	50	43	34	25
Scrub	25	21	17	12

Land cover	Hillslope Manning's n ($s\ m^{-1/3}$)			
	Unburned	Low severity	Moderate severity	High severity
Deciduous forest	0.4	0.199	0.06	0.017
Evergreen forest	0.8	0.199	0.058	0.017
Mixed forest	0.6	0.199	0.058	0.017
Scrub	0.055	0.01	0.005	0.003

Channel Manning's n : 0.035	
Total rainfall depth (mm)	
Rainfall representation	ZION
Uniform	30.22
Type II watershed	30.22
Type II burned area	42.04
DHR radar (watershed average)	30.22
Monsoon	13.18

National Monument (BAND) in north-western New Mexico (Fig. 1). USGS stream gauges were chosen as the outlets for both watersheds in order to compare modelling results with gauge records.

The outlet of North Creek is outside Zion, but much of the upper watershed is in the Park. The watershed is 24 383 ha and ranges from 887 to 2856 m above sea level. The hydrogeomorphic regime of Zion National Park is characterised by steep slopes and easily eroded soils. Half of the soil complexes within the park are rock, and 80% have high erosion potential. Bedrock and slickrock exposures are common (National Park Service 2004). According to the STATSGO database, North Creek contains four soil map units (Natural Resources Conservation Service 2013). One map unit is 80% rock outcrop, and the remaining dominant soils have K factors ranging between 0.0066 and 0.065 $t\ ha\ h\ ha^{-1}\ MJ^{-1}\ mm^{-1}$ and saturated hydraulic conductivities ranging from 1.51 to 508.10 $mm\ h^{-1}$. The watershed is generally round in shape, with two large forks that meet near the outlet of the watershed. According to Moody and Martin (2009), the watershed is within the Arizona medium-rainfall type, which has a 2-year 30-min intensity of between 20 and 36 $mm\ h^{-1}$.

In June of 2006, the Kolob fire burned 7135 ha in and around Zion, including ~12% of the North Creek watershed. Most of the burned area was climax pinyon–juniper woodland (National Park Service 2006). On 1 August 2007, a convective storm cell delivered up to 75–100 mm of rain in ~90 min on portions of the watershed, causing major flooding downstream (Sharrow 2012). The North Creek USGS stream gauge was destroyed by the flood, but an indirect measurement performed by USGS

estimated a peak flow of 382 $m^3\ s^{-1}$ (13 500 $feet^3\ s^{-1}$) with 15% confidence intervals. According to the DHR radar analysis of the storm, the average rainfall depth over the entire watershed was 30 mm, which correlates approximately to a 10-year return period event according to the National Oceanic and Atmospheric Administration's (NOAA) Atlas 14 (NOAA 2013).

The Frijoles Canyon watershed is almost entirely contained within Bandelier National Monument. The upper watershed at the Valles Caldera is covered in subalpine forest, whereas the lower watershed is a riparian forest within a narrow canyon at the outlet near the Park's Visitor Centre (Muldavin *et al.* 2011). The watershed is 4778 ha and ranges between 1626 and 3202 m above sea level. Bandelier also contains deeply incised steep-walled canyons (such as Frijoles Canyon) along with broad mesa tablelands (National Park Service 2011). According to the STATSGO database, Frijoles Canyon contains three soil map units (Natural Resources Conservation Service 2013). One map unit is 48% rock outcrop, and the dominant soils have K factors ranging between 0.0026 and 0.072 $t\ ha\ h\ ha^{-1}\ MJ^{-1}\ mm^{-1}$ and saturated hydraulic conductivities ranging from 0.00 to 508.10 $mm\ h^{-1}$. The watershed is long and narrow, with one main channel and small side channels throughout the canyon. According to Moody and Martin (2009), the watershed is also within the Arizona medium-rainfall type.

In June and July of 2011, the Las Conchas fire burned 63 400 ha in the Jemez Mountains. At the time, it was the largest fire in New Mexico state history, and burned over areas previously burned by the Dome fire of 1996 and the Cerro Grande fire of 2000 (Tillery *et al.* 2011). Over 90% of the Frijoles Canyon watershed was burned, and the middle of

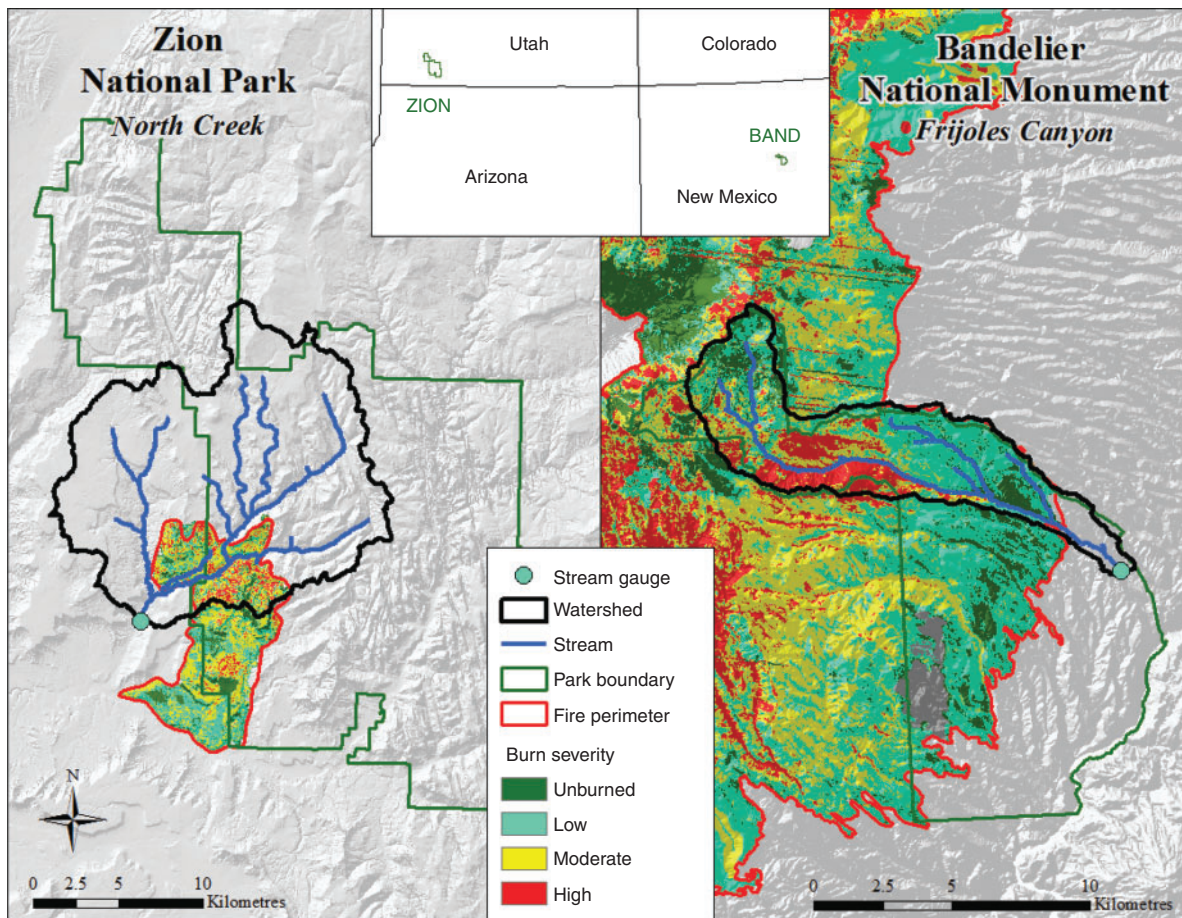


Fig. 1. Locations of the two sites in this study: the North Creek watershed (24 383 ha) in Zion National Park (ZION) and the Frijoles Canyon watershed (4778 ha) in Bandelier National Monument (BAND). Burn severity maps are shown for the 2006 Kolob Fire at ZION (burn area of 7135 ha) and the 2011 Las Conchas Fire at BAND (burn area of 63 400 ha).

the watershed was especially damaged with high-severity burns. Flooding in the watershed followed an intense rainstorm on 21 August 2011. The two rain gauges in the watershed recorded 32 and 70 mm respectively over the course of ~150 min, and the flood destroyed the USGS stream gauge at the watershed outlet. According to indirect measurements performed by the National Park Service and the USGS, the peak flow at the stream gage was $198 \text{ m}^3 \text{ s}^{-1}$ with 25% confidence intervals ($7000 \text{ feet}^3 \text{ s}^{-1}$; Monroe 2012). The DHR radar analysis showed an average rainfall depth of 54 mm over the watershed, correlating to approximately a 25-year return period event according to the NOAA Atlas 14 (NOAA 2013).

Rainfall representation using KINEROS2/AGWA

The two post-fire rainfall-runoff events (1 August 2007 at North Creek and 21 August 2011 at Frijoles Canyon) were modelled using KINEROS2 within AGWA. AGWA changes the original land-cover layer, from which it obtains parameters for KINEROS2, to represent a post-fire landscape. Changes in Manning's roughness coefficient and percentage cover, all derived from Canfield *et al.* (2005) are used (Table 1). Saturated hydraulic conductivity of the soil layer is also altered as a

function of changes to percentage cover, according to the following exponential equation:

$$K_{s\text{post-fire}} = K_{s\text{pre-fire}} \times (e^{0.0105C}) \times (1 - I)$$

where K_s is saturated hydraulic conductivity, C is percentage cover, and I is percentage of impervious cover of the soil (Stone *et al.* 1992). Input soil erosion parameters including splash and cohesion coefficients (derived from the Universal Soil Loss Equation K values for each soil unit from the STATSGO database) are not currently changed in AGWA. In this present study, burn severity maps from the Kolob and Las Conchas fires were used to change land cover in AGWA to represent the post-fire landscapes present in the study sites.

To test the effect of varying rainfall representation on accurately reproducing peak flow, four rainfall representations were modelled in KINEROS2/AGWA for each of the two storms. The first representation had uniform intensity over the entire watershed (Fig. 2), with a total depth equal to the watershed average storm depth according to the DHR radar data. The second representation had a Type II intensity distribution as outlined in Soil Conservation Service (SCS 1972) over

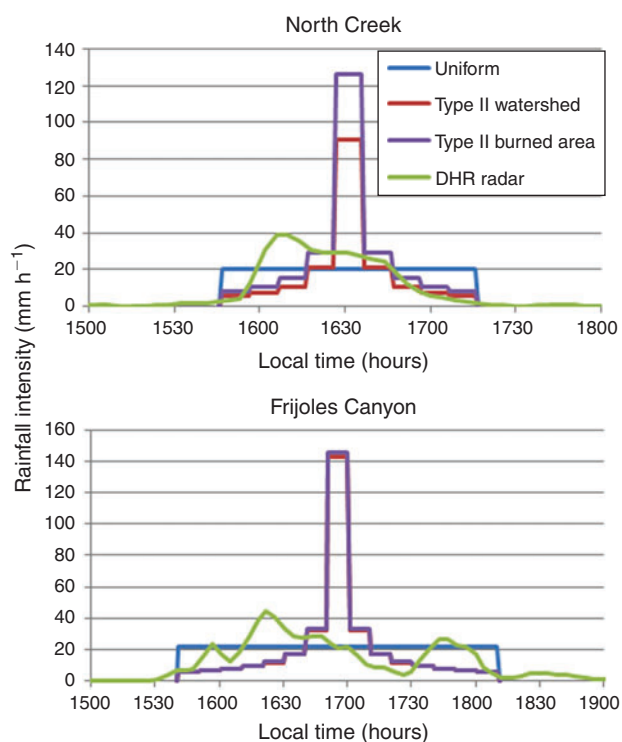


Fig. 2. Hyetographs of storms modelled to test the effect of varying rainfall representation on modelled peak flow. DHR, digital hybrid reflectivity.

the entire watershed with the same total depth as the first representation. A Type II distribution is characterised by low-intensity rainfall at the beginning of the storm that gradually becomes stronger until peak intensity is achieved in the middle of the storm before tapering off to low intensity by the end of the storm. The third representation also had a Type II intensity distribution, but rained only over the burned areas of the watershed, with a depth equal to the DHR-derived rainfall average over only the burned area. The fourth representation used the DHR radar input, which provided a unique hyetograph for each 1 km by 1 degree radial radar pixel over the watershed according to the 4–5-min interval radar scans throughout the storm. For North Creek, data from the KICX Cedar City, Utah station was used, which is ~30 km from the watershed. Data from KABX Albuquerque, New Mexico, was used for modelling at Frijoles Canyon, which is ~90 km from the watershed. At both watersheds, mountain beam blockage is low from their respective radar stations: the lowest unblocked beam used for precipitation measurement averages 1.46 m at North Creek and 0.95 m at Frijoles Canyon. Both stations use Gaussian model adaptive processing filters to reduce ground clutter (Maddox *et al.* 2002; Ice *et al.* 2007). For all simulations, a monsoonal Z–R relationship was used:

$$Z = 300R^{1.4}$$

where Z is a reflectivity factor and R is rainfall. Spatial input data for KINEROS2 were reprojected into the azimuthal projection of the radar (with a resolution of 1 km by 1 degree) centred at the radar location in order to maintain spatial accuracy of the radar grid cells. The storm durations obtained from the DHR radar

representations at each study site were used in the other three representations to make all durations equal (90 min for North Creek, 150 min for Frijoles Canyon).

To measure the effect of varying rainfall representation on predicting areas at risk of flooding and erosion, the DHR radar representation was not considered. Because reproducing the magnitude of an event is a modelling exercise inherently done after the event, radar data from the event would likely be available to the modeller. However, prediction of at-risk areas is done before a rainfall-runoff event, and therefore it is not practical to consider the radar representation for this goal. Therefore, only the uniform, Type II entire watershed, and Type II burned area representations were used for predictive purposes, along with a design storm typical of convective monsoon storms. This design storm was a Type II 2-year, 30-min storm over the entire watershed, with a unique rainfall depth for each study site determined from the NOAA Atlas 14 (NOAA 2013). At Zion, the 2-year, 30-min storm had a depth of 13 mm (compared with the uniform and Type II depth of 30 mm and the Type II burned area depth of 42 mm), and at Bandelier, the 2-year, 30-min storm had a depth of 18 mm (compared with the uniform/Type II depth of 54 mm and the Type II burned area depth of 55 mm). Each of the four rainfall representations were modelled on both a pre- and post-fire landscape on each of the two watersheds. The percentage change in KINEROS2/AGWA outputs for peak flow and sediment yield between the pre- and the post-fire simulations were used as metrics to predict at-risk areas.

Results and discussion

Reproducing post-fire peak flow

When comparing the peak flow given by the four rainfall representations at both study sites, the representation of uniform rainfall intensity over the entire watershed was clearly the least accurate (Fig. 3). At both North Creek and Frijoles Canyon, the uniform representation severely underestimated peak flow: in North Creek, peak flow was $2.53 \text{ m}^3 \text{ s}^{-1}$ compared with the USGS estimate of $382 \text{ m}^3 \text{ s}^{-1}$, and in Frijoles Canyon peak flow was $103 \text{ m}^3 \text{ s}^{-1}$ compared with the USGS estimate of $198 \text{ m}^3 \text{ s}^{-1}$. Uniform rainfall intensity generally underestimates peak flow even in unburned conditions (Dunkerley 2012), so these results are unsurprising. This consistent underprediction, likely because peak flow is driven by short periods of high-intensity rainfall that are missing in uniform rainfall intensity representations, also points to the danger in using a uniform rainfall intensity when using modelling results for such goals as predicting the magnitude of potential flood events in absolute terms.

The two Type II rainfall representations were more similar to USGS estimates than the uniform representation, but under-predicted peak flow at North Creek and over-predicted it at Frijoles Canyon. This improvement from the uniform representation is attributable to the temporal variability in the Type II storms, giving the representation increments of high-intensity rainfall that have been shown to drive post-fire runoff. The fact that the Type II storms under-predicted in one site but over-predicted in the other is probably due to the differing spatial relationships in the two watersheds between the amount of

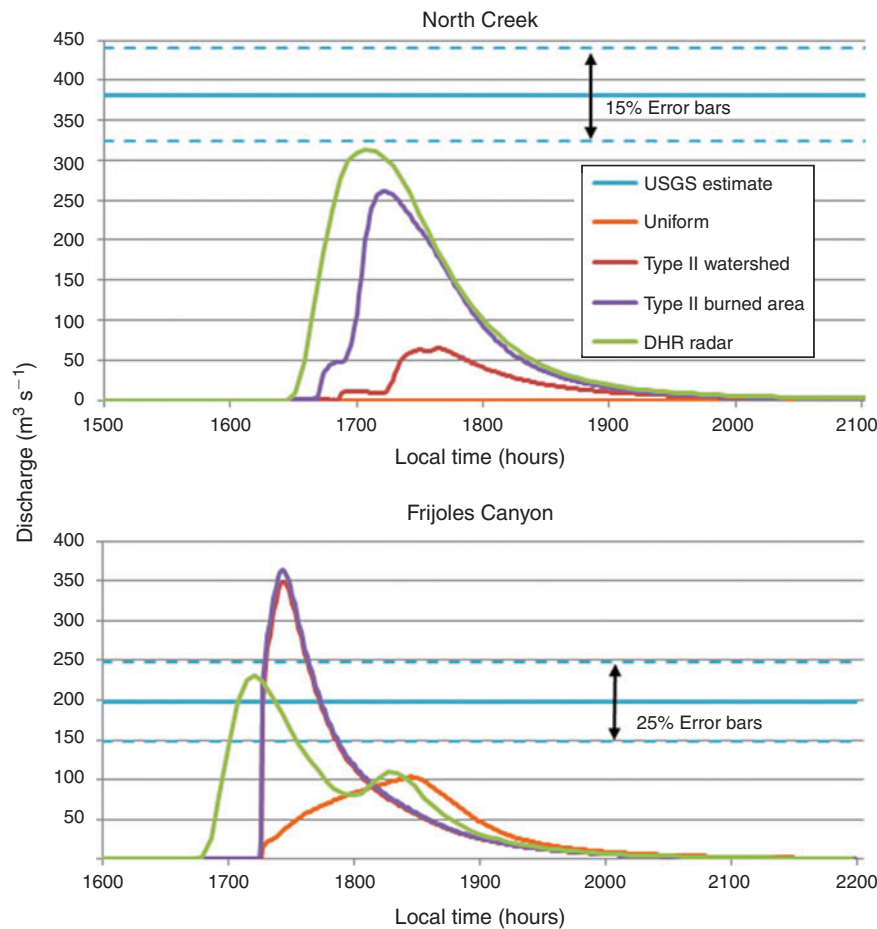


Fig. 3. Hydrographs for modelled storms. ‘Uniform’ represents uniform rainfall intensity over the entire watershed, Type II Watershed is an SCS (Soil Conservation Service) Type II distribution (SCS 1972) over the entire watershed, Type II Burned Area is an SCS Type II distribution over just the burned area, and DHR (digital hybrid reflectivity) Radar is data for the actual storm (1 August 2007 at Zion and 21 August 2011 at Bandelier). The US Geological Survey (USGS) peak flow and uncertainty estimates are based on post-flood indirect measurements and analysis. DHR, digital hybrid reflectivity.

burned area and the location of high-intensity rainfall (Fig. 4). In North Creek, only 12% of the watershed burned, yet the measured peak flow at the stream gauge was very high. This is because the high-intensity rainfall fell directly over the burned area, causing that high peak flow. The Type II representation over the entire watershed underpredicted peak flow greatly (83% drop from USGS estimate), whereas the Type II representation over just the burned area did better (32% drop from USGS estimate). This supports the argument that very-high-intensity rainfall fell directly over the burned area, whereas rainfall on the unburned area had little impact on the peak flow. At Frijoles Canyon, most of the watershed burned, so the difference in rainfall representation and subsequent peak flow was small between the two Type II representations (the Type II watershed representation showed a 76% increase from the USGS estimate, whereas the Type II burned area representation showed an 84% increase). As both representations overpredicted peak flow, it can be assumed that the actual storm did not see as much high-intensity rainfall over the severely burned areas as the

modelled storms. This assumption is supported by looking at the radar storm totals (Fig. 4), which show more uniform rainfall totals over the Frijoles watershed than the North Creek watershed. In North Creek, the higher rainfall totals are clearly centred over the burned area, whereas in Frijoles Canyon, the areas with the highest rainfall totals did not greatly coincide with areas of high burn severity. The greater uniformity in rainfall over Frijoles Canyon could partially be due to the fact that it is a smaller watershed, and therefore the spatial resolution of the radar grids is coarser compared with the size of the watershed. However, a smaller watershed will inherently have more uniform rainfall, especially with the small monsoonal storms modelled in the present study.

In both watersheds, the simulations with the DHR radar representations showed the most comparable peak flows with the USGS estimates. In North Creek, the DHR underpredicted peak flow by 18%, and at Frijoles Canyon it overpredicted peak flow by 17%. This improvement in modelling results can be largely attributed to the more accurate rainfall representation

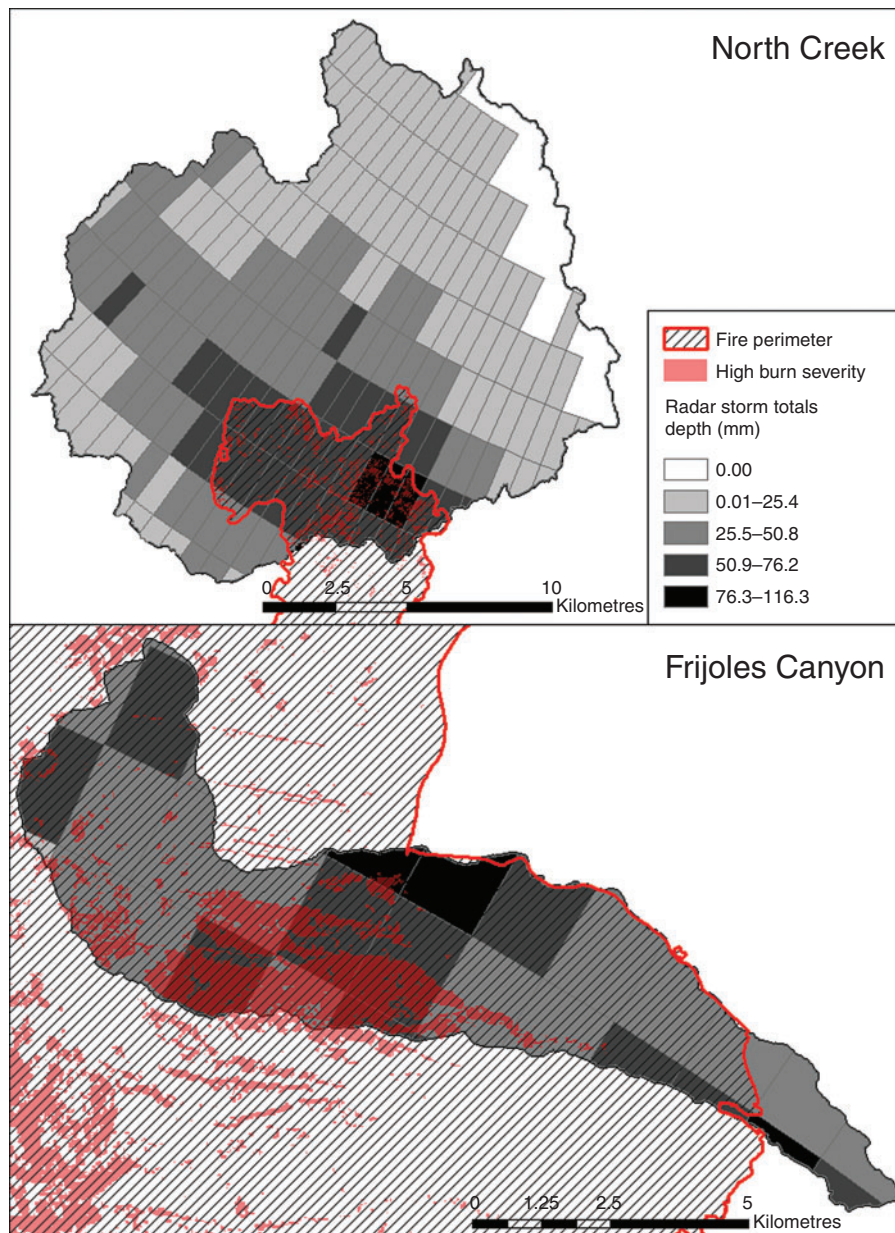


Fig. 4. Storm total precipitation for post-fire floods according to NEXRAD radar products.

that the radar provided. It was the only representation considered in the present study that varied both spatially and temporally throughout the course of the storm. It also points to the importance of rainfall representation in model performance. KINEROS2/AGWA was not calibrated for either watershed in this study and still showed peak flows within 20% of USGS peak flow measurements (indirect measurements that had 15 and 25% error themselves) using the more accurate DHR radar rainfall input. In contrast, the less-dynamic rainfall representations showed peak flows much further from the USGS estimates.

Although the present study focussed on the differences in rainfall representation within the model, there are other parameters, which although left constant for all modelling scenarios, surely influenced actual runoff response in the two watersheds.

Initial soil moisture, one such parameter, can greatly influence runoff timing and magnitude in post-fire runoff events (Onda *et al.* 2008; Moody and Ebel 2014). Initial soil moisture for all model simulations was kept at the AGWA default of 0.2 (representing the fraction of filled pore space), but in reality may have been higher. An adjacent watershed to North Creek experienced heavy flooding 4 days before the flood modelled in this study, although rain gauge records in Frijoles Canyon show minor rainfall in the week leading up to the flood. Rainfall in the days leading up to the major flood event could cause higher initial soil moisture content, which in turn could lead to quicker soil saturation and thus earlier and higher runoff rates. Initial vegetation cover values also influence runoff response. In AGWA, conditions in the soil-vegetation complex are

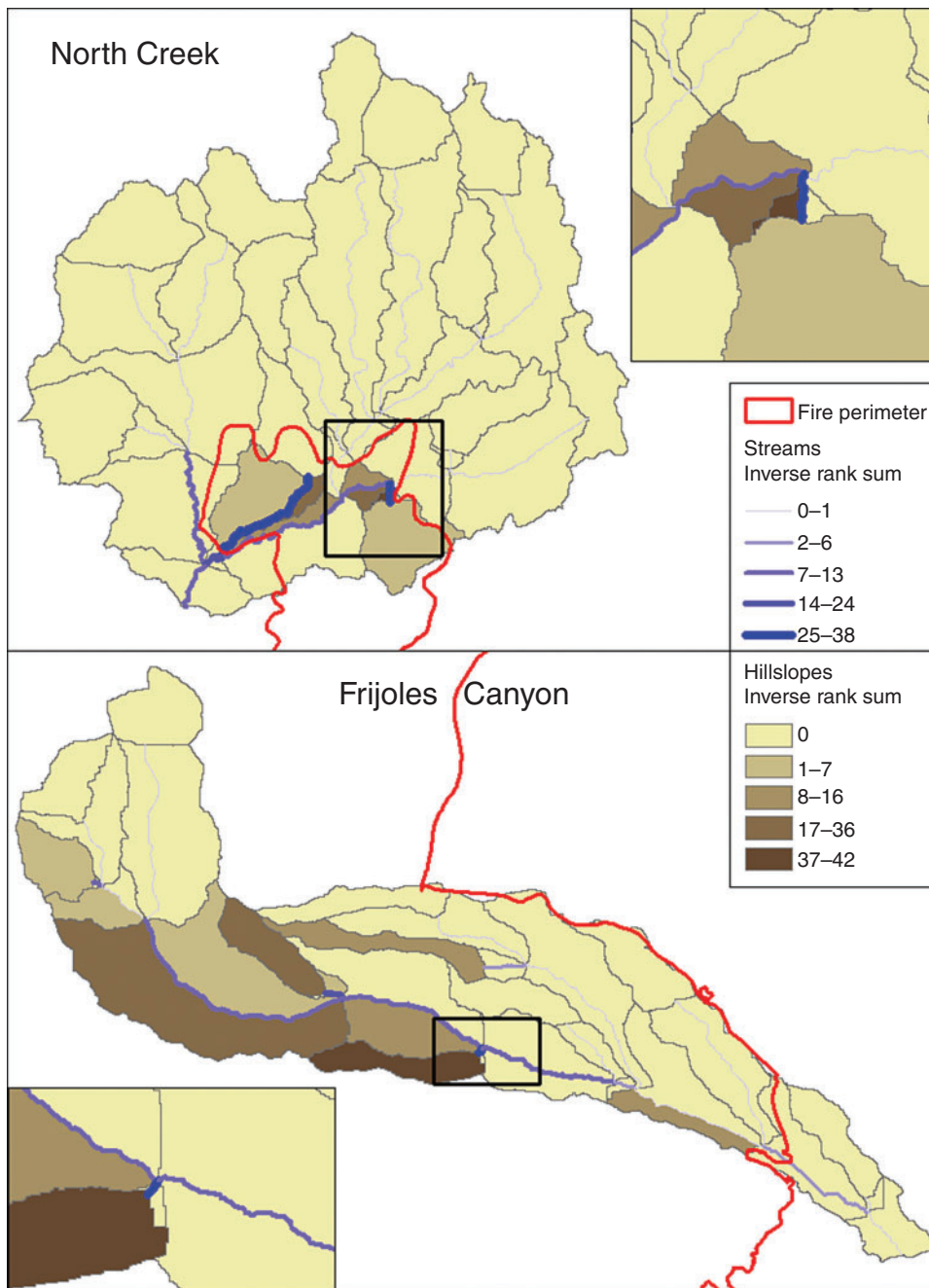


Fig. 5. Map of high-risk hillslopes and stream channels. The inverse ranks are summed for the stream channels and hillslopes, showing the highest five relative changes for peak flow and sediment yield respectively.

time-invariant and do not take into account seasonal or other changes in cover. As both these runoff floods were in summer, cover may have been higher than represented in AGWA. However, the reduction in cover caused by the fires is represented in AGWA (Table 1). Despite possible misrepresentations of initial conditions, the results illustrated that KINEROS2/AGWA can perform reasonably well with the default parameterisation with improved rainfall representation.

Prediction of high-risk hillslopes and stream reaches

In order to determine if rainfall representation changed the model’s predicted areas of high risk, stream reaches and hillslopes were ranked from highest to lowest percentage change from pre- to post-fire for each rainfall representation. Change in peak flow was used for stream reaches while change in sediment yield was used for hillslopes. One possible high-risk criterion is

Table 2. Spearman's rank correlation coefficients for four modelled storms at both study sites

For each watershed, numbers in the upper right represent correlation coefficients for peak flow on stream reaches between different rainfall representations, while numbers in the lower left represent correlation coefficients for sediment yield on hillslopes. Monsoon is a 2-year, 30-min design storm typical of convective monsoon storms. ZION, Zion National Park; BAND, Bandelier National Monument

North Creek (ZION)			
Peak flow for stream reaches			
Type II burned area	0.76	0.66	0.46
0.90	Type II watershed	0.84	0.73
0.89	0.98	Uniform	0.88
0.89	0.97	0.99	Monsoon
Sediment yield for hillslopes			
Frijoles Canyon (BAND)			
Peak flow for stream reaches			
Type II burned area	1.00	0.83	0.83
1.00	Type II watershed	0.82	0.85
0.80	0.81	Uniform	0.62
0.67	0.68	0.70	Monsoon
Sediment yield for hillslopes			

the inverse rank sum, which combines the effects of all rainfall representations. To calculate inverse rank sums, ranks were given to each watershed element (stream reaches and hillslopes) according to their relative change from pre- to post-fire. The watershed element with the highest relative change for each rainfall representation was given a rank of one. Points were then assigned inversely to the watershed elements that ranked one through five for each rainfall representation so that a watershed element with a ranking of one was given five points. These points were then summed across all rainfall representations for each watershed to give the inverse rank sum for each watershed element (Fig. 5).

Another high-risk criterion that treats each rainfall representation separately is to use Spearman's rank correlation coefficient as outlined in McBean and Rovers (1998). Spearman's rank correlation coefficient measures the statistical dependence between two ordinal variables, and thus can be used to compare the difference between two sets of rankings. Using the correlation coefficient, rankings of relative change between pre- and post-fire sediment yield for both hillslope and stream channel elements were compared (Table 2). Only hillslopes within the burned area and stream channels within or downstream of the burned area were considered when calculating the coefficients, because unburned hillslopes and stream channels show no change pre- to post-fire, and therefore would all have the exact same relative change ranking regardless of rainfall representation. If burned and unburned hillslopes and stream channels were included in the correlation coefficient calculation, the coefficients would show misleadingly correlated values, because all unburned hillslopes and channels would have matching rankings across all rainfall representations. This would be especially true for North Creek, which had a low ratio of burned area to unburned area within the watershed.

In general, Spearman's coefficients were high, pointing to agreement in rankings across the different rainfall representations (a coefficient of 1 corresponds to a perfect agreement, whereas a ranking of -1 corresponds to an inverse agreement). At North Creek, the average coefficient for stream reaches was 0.72, and the average for hillslopes was 0.94. At Frijoles Canyon, the average for stream reaches was 0.82, and the average for hillslopes was 0.78. These high coefficients suggest that KINEROS2 may not be sensitive to change in rainfall representation when predicting areas of high relative change pre- to post-fire. One reason for the lack of model sensitivity could be the spatial uniformity over burned areas of all the rainfall representations modelled for this section of the study. As within each rainfall representation equal amounts of rain were applied to every portion of the burned area in each watershed (even though each representation had a different intensity distribution), each burned hillslope and stream reach received exactly the same amount of rain within each model run. Therefore, differences in ground conditions, such as burn severity, slope or soil type must have driven the major variations of peak flow or sediment yield between stream reaches and hillslopes. Because these differences in topographical, soils and land-cover features remained constant for all rainfall representations, they undoubtedly drove the hydrological results for all model runs, regardless of rainfall representation.

The fact that rainfall representation does not greatly affect prediction of high-risk areas is also important in a rapid post-fire assessment situation, where the use of predictive models is done without knowledge of the characteristics of a future storm that might cause flooding and erosion. According to these results, such knowledge may not be necessary because all representations highlight the same stream channels and hillslopes that are at highest risk of flooding and erosion. An analysis of multiple rainfall representations would be helpful to gain a larger sample size as done in this study, but may not always be necessary in rapid-assessment situations. However, models may still be very sensitive to input parameters other than rainfall, which could change the prediction of high-risk areas. A large watershed such as North Creek in which only a small area was burned is very likely to be sensitive to parameters such as initial moisture content. However, by keeping all non-rainfall parameters constant throughout all model runs, this study focusses solely on changes in rainfall representation.

Conclusions

Peak discharge varied greatly with different rainfall representations at both study sites when other input parameters to KINEROS2 were kept constant at default AGWA values. This illustrates that accurate rainfall depiction is critical for matching modelled post-fire peak flow to observed values. The DHR radar rainfall representation indicates that model runs with high-quality rainfall data can provide results within 20% of indirect measurement estimates even in the absence of calibration steps. Methods that rely on spatially or temporally uniform rainfall can skew model results greatly.

Rainfall representation had less effect on identifying areas of high risk (i.e. pre- to post-fire relative change) at both study sites. This supports the continued use of hydrological models in

predictive situations where rainfall characteristics are unknown. However, adjustments of non-rainfall parameters were not analysed in this study but may affect model sensitivity to prediction of at-risk locations. Design storm representations can still guide emergency response teams and land managers in identifying watershed areas and channels most at risk if those areas were to receive rainfall. As actual storms tend to produce local concentrations of high-intensity rainfall (bursts), such predictions may not prove to be accurate for any given storm. However, without a reliable way to predict the location of these bursts of heavy rainfall, assuming rainfall on all burned areas of the watershed allows models to evaluate which areas would hypothetically see the most damage.

Acknowledgements

Thank you to Zion National Park hydrologist David Sharrow, Southern Colorado Plateau Inventory and Monitoring Network hydrologist Stephen Monroe, Bandelier staff Brian Jacobs and Kay Beeley, and Craig Allen of the USGS for their support of this project and providing invaluable data. Thank you also to Brian Mcinerney of NOAA for providing and interpretation of radar data. Financial support provided by the National Park Service via an Interagency Agreement is also gratefully acknowledged.

References

- Banta RM, Barker Schaaf C (1987) Thunderstorm genesis zones in the Colorado Rocky Mountains as determined by traceback of geosynchronous satellite images. *Monthly Weather Review* **115**(2), 463–476. doi:10.1175/1520-0493(1987)115<0463:TGZITC>2.0.CO;2
- Canfield EH, Burns IS, Goodrich DC (2005) Selection of parameters values to model post-fire runoff and sediment transport at the watershed scale in south-western forests. In 'Watershed Management Conference Proceedings', 19–22 July 2005, Williamsburg, VA. (Ed. GE Moglen) American Society of Civil Engineers (Williamsburg, VA)
- Cannon SH, Gartner JE, Wilson RC, Bowers JC, Laber JL (2008) Storm rainfall conditions for floods and debris flows from recently burned areas in south-western Colorado and southern California. *Geomorphology* **96**(3–4), 250–269. doi:10.1016/J.GEOMORPH.2007.03.019
- Chen F, Warner TT, Manning K (2001) Sensitivity of orographic moist convection to landscape variability: a study of the Buffalo Creek, Colorado, flash flood case of 1996. *Journal of the Atmospheric Sciences* **58**(21), 3204–3223. doi:10.1175/1520-0469(2001)058<3204:SOOMCT>2.0.CO;2
- Dunkerley D (2012) Effects of rainfall intensity fluctuations on infiltration and runoff: rainfall simulation on dryland soils, Fowlers Gap, Australia. *Hydrological Processes* **26**(15), 2211–2224. doi:10.1002/HYP.8317
- Faurès J, Goodrich DC, Woolhiser DA, Sorooshian S (1995) Impact of small-scale spatial rainfall variability on runoff modeling. *Journal of Hydrology* **173**(1–4), 309–326. doi:10.1016/0022-1694(95)02704-S
- Foltz RB, Robichaud PR, Rhee H (2009) A synthesis of post-fire road treatments for BAER teams. USDA Forest Service, Rocky Mountain Research Station, Paper RMRS-GTR-228. (Fort Collins, CO)
- Garcia M, Peters-Lidard CD, Goodrich DC (2008) Spatial interpolation of precipitation in a dense gauge network for monsoon storm events in the south-western United States. *Water Resources Research* **44**(5), doi:10.1029/2006WR005788
- Goodrich DC, Faurès J, Woolhiser DA, Lane LJ, Sorooshian S (1995) Measurement and analysis of small-scale convective storm rainfall variability. *Journal of Hydrology* **173**(1–4), 283–308. doi:10.1016/0022-1694(95)02703-R
- Goodrich DC, Lane LJ, Shillito RM, Miller SN, Syed KH, Woolhiser DA (1997) Linearity of basin response as a function of scale in a semiarid watershed. *Water Resources Research* **33**(12), 2951–2965. doi:10.1029/97WR01422
- Goodrich DC, Burns IS, Unkrich C, Semmens D, Guertin DP, Hernandez M, Yatheendradas S, Kennedy J, Levick L (2012) KINEROS2/AGWA: model use, calibration, and validation. *Transactions of the ASABE* **55**(4), 1561–1574. doi:10.13031/2013.42264
- Hardegree S, Van Vactor S, Healy K, Alonso C, Bonta J, Bosch D, Fisher D, Goodrich D, Harmel D, Steiner J, Van Liew M (2003) Multi-watershed evaluation of WSR-88D (NEXRAD) radar precipitation products. In 'Proceedings of the 1st Interagency Conference on Research in the Watersheds', 27–30 October 2003, Benson, AZ. (Eds KG Renard, S McElroy, W Gburek, E Canfield, RL Scott) USDA Agricultural Research Service, pp. 486–491. (Benson, AZ)
- Hernandez M, Miller SN, Goodrich DC, Goff BF, Kepner WG, Edmonds CM, Jones KB (2000) Modeling runoff response to land-cover and rainfall spatial variability in semi-arid watersheds. In 'Monitoring ecological condition in the western United States.' (Eds SS Sandhu, BD Melzian, ER Long, WG Whitford, BT Walton) pp. 285–298. (Springer: New York)
- Hossain F, Anagnostou EN, Dinku T, Borga M (2004) Hydrological model sensitivity to parameter and radar rainfall estimation uncertainty. *Hydrological Processes* **18**(17), 3277–3291. doi:10.1002/HYP.5659
- Ice RL, Rhoton RD, Saxion DS, Ray CA, Patel NK, Warde DA, Free AD, Boydstun OE, Berkowitz DS, Chrisman JN, Hubbert JC, Kessinger C, Dixon M, Torres S (2007) Optimizing clutter filtering in the WSR-88D. Available at <https://ams.confex.com/ams/pdfpapers/116863.pdf> [Verified 19 May 2015]
- Jorgensen DP, Hanshaw MN, Schmidt KM, Laber JL, Staley DM, Kean JW, Restrepo PJ (2011) Value of a dual-polarized gap-filling radar in support of southern California post-fire debris-flow warnings. *Journal of Hydrometeorology* **12**(6), 1581–1595. doi:10.1175/JHM-D-11-05.1
- Kean JW, Staley DM, Cannon SH (2011) *In situ* measurements of post-fire debris flows in southern California: comparisons of the timing and magnitude of 24 debris-flow events with rainfall and soil moisture conditions. *Journal of Geophysical Research: Earth Surface* **116**(F4), F04019. doi:10.1029/2011JF002005
- Lambourne JJ, Stephenson D (1987) Model study of the effect of temporal storm distributions on peak discharges and volumes. *Hydrological Sciences Journal* **32**(2), 215–226. doi:10.1080/02626668709491179
- Maddox RA, Zhang J, Gourley JJ, Howard KW (2002) Weather radar coverage over the contiguous United States. *Weather and Forecasting* **17**, 927–934. doi:10.1175/1520-0434(2002)017<0927:WRCOTC>2.0.CO;2
- McBean EA, Rovers FA (1998) 'Statistical procedures for analysis of environmental monitoring data and risk assessment, Vol. 3.' (Prentice Hall PTR: Upper Saddle River, NJ)
- Milly PCD, Eagleson PS (1988) Effect of storm scale on surface runoff volume. *Water Resources Research* **24**(4), 620–624. doi:10.1029/WR024I004P00620
- Monroe S (2012) Rito de los Frijoles – Post Las Conchas fire floods – 2011. DOI National Park Service, Bandelier National Monument. (Los Alamos, NM)
- Moody JA (2011) An analytical method for predicting post-wildfire peak discharges. DOI USGS Investigations Report 2011–5236. (Reston, VA)
- Moody JA, Ebel BA (2014) Infiltration and runoff generation processes in fire-affected soils. *Hydrological Processes* **28**(9), 3432–3453. doi:10.1002/HYP.9857
- Moody JA, Martin DA (2001) Post-fire, rainfall intensity–peak discharge relations for three mountainous watersheds in the western USA. *Hydrological Processes* **15**(15), 2981–2993. doi:10.1002/HYP.386
- Moody JA, Martin DA (2009) Synthesis of sediment yields after wildland fire in different rainfall regimes in the western United States. *International Journal of Wildland Fire* **18**(1), 96–115. doi:10.1071/WF07162

- Moody JA, Shakesby RA, Robichaud PR, Cannon SH, Martin DA (2013) Current research issues related to post-wildfire runoff and erosion processes. *Earth-Science Reviews* **122**, 10–37. doi:10.1016/J.EARSCIREV.2013.03.004
- Morin E, Goodrich DC, Maddox RA, Gao X, Gupta HV, Sorooshian S (2006) Spatial patterns in thunderstorm rainfall events and their coupling with watershed hydrological response. *Advances in Water Resources* **29**(6), 843–860. doi:10.1016/J.ADVWATRES.2005.07.014
- Muldavin E, Kennedy A, Jackson C, Neville T (2011) Vegetation classification and map – Bandelier National Monument. DOI National Park Service, Natural Resource Technical Report NPS/SCPN/NRTR 2011/438. (Fort Collins, CO)
- National Oceanic and Atmospheric Administration (NOAA) (2013) NOAA Atlas 14 point precipitation frequency estimates. Available at http://hdsc.nws.noaa.gov/hdsc/pfds/pfds_map_cont.html?bkmrk=nm [Verified 18 May 2015]
- National Park Service (2004) Zion National Park fire management plan: environmental assessment/assessment of effect. DOI National Park Service, Zion National Park. (Springdale, UT)
- National Park Service (2006) Zion National Park fire and aviation management annual report 2006. DOI National Park Service, Zion National Park. (Springdale, UT)
- National Park Service (2011) Vegetation classification and map Bandelier National Monument. DOI National Park Service, Natural Resource Technical Report NPS/SCPN/NRTR-2011/438 (Fort Collins, CO)
- Natural Resources Conservation Service (2013) Web soil survey. Available at <http://websoilsurvey.nrcs.usda.gov/> [Verified 18 May 2015]
- Onda Y, Dietrich WE, Booker F (2008) Evolution of overland flow after a severe forest fire, Point Reyes, California. *Catena* **72**(1), 13–20. doi:10.1016/J.CATENA.2007.02.003
- Robichaud PR, Elliot WJ, Pierson FB, Hall DE, Moffet CA, Ashmun LE (2007) Erosion Risk Management Tool (ERMiT) user manual (version 2006.01. 18). USDA Forest Service, Rocky Mountain Research Station, General Technical Report RMRS-GTR-188. (Fort Collins, CO)
- Schaffner M, Unkrich C, Goodrich D (2010) Application of the KINEROS2 site-specific model to south-central NY and north-east PA: forecasting gaged and ungaged fast-responding watersheds. National Weather Service Forecast Office, Eastern Region Technical Attachment No. 2010–01. (Binghamton, NY)
- Schröter K, Llort X, Velasco-Forero C, Ostrowski M, Sempere-Torres D (2011) Implications of radar rainfall estimates uncertainty on distributed hydrological model predictions. *Atmospheric Research* **100**(2–3), 237–245. doi:10.1016/J.ATMOSRES.2010.08.014
- Sharrow D (2012) A summary of the July 27 and August 1, 2007 Floods in Zion National Park. DOI National Park Service, Zion National Park. (Springdale, UT)
- Singh VP (1998) Effect of the direction of storm movement on planar flow. *Hydrological Processes* **12**(1), 147–170. doi:10.1002/(SICI)1099-1085(199801)12:1<147::AID-HYP568>3.0.CO;2-K
- Singh VP, Woolhiser DA (2002) Mathematical modeling of watershed hydrology. *Journal of Hydrologic Engineering* **7**(4), 270–292. doi:10.1061/(ASCE)1084-0699(2002)7:4(270)
- Soil Conservation Service (SCS) (1972) 'National engineering handbook, hydrology section. Vol. 4.' (USDA Soil Conservation Service: Washington DC)
- Stone JJ, Lane LJ, Shirley ED (1992) Infiltration and runoff simulation on a plane. *Transactions of the ASABE* **35**(1), 161–170. doi:10.13031/2013.28583
- Tao K, Barros P (2010) Using fractal downscaling of satellite precipitation products for hydrometeorological applications. *Journal of Atmospheric and Oceanic Technology* **27**, 409–427. doi:10.1175/2009JTECHA1219.1
- Tillery AC, Darr MJ, Cannon SH, Michael JA (2011) Post-wildfire preliminary debris flow hazard assessment for the area burned by the 2011 Las Conchas Fire in north-central New Mexico. DOI US Geological Survey Open-File Report 2011–1308. (Reston, VA)
- Tryhorn L, Lynch A, Abramson R, Parkyn K (2008) On the meteorological mechanisms driving post-fire flash floods: a case study. *Monthly Weather Review* **136**, 1778–1791. doi:10.1175/2007MWR2218.1
- Woolhiser DA, Goodrich DC (1988) Effect of storm rainfall intensity patterns on surface runoff. *Journal of Hydrology* **102**(1–4), 335–354. doi:10.1016/0022-1694(88)90106-0
- Wright DB, Smith JA, Baeck ML (2014) Critical examination of area reduction factors. *Journal of Hydrologic Engineering* **19**(4), 769–776. doi:10.1061/(ASCE)HE.1943-5584.0000855
- Yatheendradas S, Wagener T, Gupta H, Unkrich C, Goodrich D, Schaffner M, Stewart A (2008) Understanding uncertainty in distributed flash flood forecasting for semiarid regions. *Water Resources Research* **44**(5), doi:10.1029/2007WR005940